Clim Dyn (2017) 48:2685–2705
DOI 10.1007/s00382-016-3232-2

Future changes to drought characteristics over the Canadian Prairie Provinces based on NARCCAP multi-RCM ensemble

M. B. Masud[1] · M. N. Khaliq[1,2] · H. S. Wheater[1]

Received: 31 December 2015 / Accepted: 7 June 2016 / Published online: 14 June 2016

Abstract This study assesses projected changes to drought characteristics in Alberta, Saskatchewan and Manitoba, the prairie provinces of Canada, using a multi-regional climate model (RCM) ensemble available through the North American Regional Climate Change Assessment Program. Simulations considered include those performed with six RCMs driven by National Center for Environmental Prediction reanalysis II for the 1981–2003 period and those driven by four Atmosphere–Ocean General Circulation Models for the 1970–1999 and 2041–2070 periods (i.e. eleven current and the same number of corresponding future period simulations). Drought characteristics are extracted using two drought indices, namely the Standardized Precipitation Index (SPI) and the Standardized Precipitation Evapotranspiration Index (SPEI). Regional frequency analysis is used to project changes to selected 20- and 50-year regional return levels of drought characteristics for fifteen homogeneous regions, covering the study area. In addition, multivariate analyses of drought characteristics, derived on the basis of 6-month SPI and SPEI values, are developed using the copula approach for each region. Analysis of multi-RCM ensemble-averaged projected changes to mean and selected return levels of drought characteristics show increases over the southern and south-western parts of the study area. Based on bi- and trivariate joint occurrence probabilities of drought characteristics, the southern regions along with the central regions are found highly drought vulnerable, followed by the southwestern and southeastern regions. Compared to the SPI-based analysis, the results based on SPEI suggest drier conditions over many regions in the future, indicating potential effects of rising temperatures on drought risks. These projections will be useful in the development of appropriate adaptation strategies for the water and agricultural sectors, which play an important role in the economy of the study area.

Keywords Drought characteristics · Copula · Multivariate frequency analysis · Multivariate homogeneity testing · Regional climate model · NARCCAP · Canadian Prairie Provinces

1 Introduction

Drought is considered to be a continuous dry weather phenomenon with abnormally low precipitation for a period ranging from several months to years. It can cause severe damage to both the natural environment and human lives. For example, the 2012–2013 U.S. drought in the Central Plains caused more than US $12 billion in damages in the U.S., while the 1995 drought in Spain and the 1982 drought in Australia cost US $4.5 and US $6 billion, respectively (Touma et al. 2015). In spite of having world's largest freshwater resources, Canada is not drought proof. Several multi-year droughts for the 1890s, 1910s, 1930s, late 1950s, early 1960s and 1980s have been reported in the southern

Electronic supplementary material The online version of this article (doi:10.1007/s00382-016-3232-2) contains supplementary material, which is available to authorized users.

✉ M. B. Masud
mbm806@mail.usask.ca

[1] Global Institute for Water Security and School of Environment and Sustainability, University of Saskatchewan, 11 Innovation Boulevard, Saskatoon, SK S7N 3H5, Canada

[2] Ocean, Coastal and River Engineering, National Research Council of Canada, 1200 Montreal Road, Building M-32, Ottawa, ON K1A 0R6, Canada

parts of the Alberta, Saskatchewan and Manitoba provinces of Canada. The drought experienced during the 1999–2004 period was the most severe over the last 100 years (Evans et al. 2011). Gross domestic product declined respectively by $2.1 and $3.6 billion in the years 2001 and 2002, with the total loss estimated over the same period amounted to $5.8 billion (Wheater and Gober 2013). Considering the massive impact of droughts, it is important to know how anticipated climate change will influence drought characteristics in this region. Projections of future droughts will be useful for the assessment of climate change impacts on water infrastructure and agriculture and in the development of efficient adaptation strategies.

The primary tool to assess future climate change is to use simulations of coupled global and regional climate models when these models are integrated from the recent past to some point in time in the future (Flato et al. 2013). Currently, regional climate models (RCMs) offer higher spatial resolution than Global Climate Models (GCMs) and therefore, RCMs can help represent many finer scale features and atmospheric processes which are not possible using GCMs (e.g. see Leung et al. 2004; Giorgi 2006; May 2008; Gao et al. 2012; Torma et al. 2015). Due to these merits of RCMs, many studies have used RCM simulations for the assessment of future changes to climatic extremes including droughts (e.g. Beniston et al. 2007; Sushama et al. 2010; Nikulin et al. 2011; Poitras et al. 2011; Gao et al. 2014; Jeong et al. 2014; Diasso and Abiodun 2015; Huang et al. 2015).

This study explores projected changes to drought characteristics and future drought risks over the Canadian Prairie Provinces of Alberta, Saskatchewan and Manitoba based on the North American Regional Climate Change Assessment Program (NARCCAP) multi-RCM ensemble. The use of multi-RCM ensemble is important to quantify various sources of uncertainties such as those due to the internal dynamics and physics of the RCMs and those due to the lateral boundary data from driving GCMs. The multi-RCM ensemble is also useful in reducing the uncertainty associated with the projections of a single model by averaging results of various models. Drought events are defined on the basis of Standardized Precipitation Index (SPI; McKee et al. 1993), which is a purely precipitation-based index, and Standardized Precipitation Evapotranspiration Index (SPEI; Vicente-Serrano et al. 2010), which is a temperature and precipitation-based index. The use of SPI and SPEI together helps to better understand the impact of future rises in temperature on drought characteristics. Drought events are characterized in terms of three associated characteristics, i.e. drought severity, duration and maximum severity. These characteristics are modelled using the univariate regional frequency analysis (RFA) approach of Hosking and Wallis (1997) and copula-based multivariate approaches. Within the multivariate frequency analysis framework, copula-based bi- and trivariate frequency analyses are performed to study projected changes to drought characteristics. Compared to univariate approaches, copula-based multivariate approaches are useful in modelling inter-dependence of drought characteristics and thus can provide more realistic information for drought risk analysis and in the identification of drought sensitive geographic regions.

Examples of previous studies wherein copula-based bivariate analysis of drought characteristics was undertaken include the studies by Serinaldi et al. (2009), Kao and Govindaraju (2010), Halwatura et al. (2015), and Masud et al. (2015). It is important to note that most of these studies were performed using observational data. Quite a few drought-related studies have also used a trivariate analysis approach. For example, Wong et al. (2010) analyzed droughts in Australia based on rainfall data categorized into three climatic states (i.e. El-Niño, Neutral and La-Niña) and using the Gumbel–Hougaard and *t*-copulas to model these states. Madadgar and Moradkhani (2013) explored drought risks under climate change using Gumbel and *t*-copula in Oregon's Upper Klamath River Basin. They found less frequent droughts in the future compared to the historical period. Ganguli and Reddy (2013) performed multivariate frequency analysis of droughts for three meteorological subdivisions of western India using multivariate copula functions and demonstrated the importance of trivariate frequency analysis, which provided significant additional insights for drought risk management over the univariate approaches. Ma et al. (2013) applied copula-based trivariate approach to investigate changing behavior of drought events in the Weihe River Basin, China.

Frequency analysis of drought characteristics has mostly been performed on the basis of non-regional univariate and/or multivariate approaches and on the basis of regional univariate approaches only. Some forms of regional multivariate approaches are beginning to emerge for other hydrometeorological variables (e.g. Chebana and Ouarda 2007; Sadri and Burn 2011; Rajsekhar et al. 2013). In the present study, both univariate and multivariate approaches are explored for the analysis of projected changes to drought characteristics on a regional basis by defining and validating homogeneous regions based on cluster analysis and multivariate L-moments, developed by Serfling and Xiao (2007), and multivariate homogeneity tests developed by Chebana and Ouarda (2007).

This paper is organized as follows: description of the study area, observed datasets, and RCM simulations used in the study are described in Sect. 2. Description of the methodology for characterizing drought events, performing univariate RFA and copula-based multivariate frequency analyses are provided in Sect. 3. Validation and boundary

forcing analysis of RCMs, development of projected changes to selected drought characteristics, and some other supporting results of the study are presented and discussed in Sect. 4, followed by the main conclusions in Sect. 5.

2 Study area, observed and model data, and the reference grid

The study area consists of Alberta, Saskatchewan and Manitoba provinces of Canada (Fig. 1). Southern parts of these provinces, particularly the Prairies ecozone, are important for agricultural activities and account for around 80 % of the Canadian agricultural production (Wheater and Gober 2013). The ecosystem of this region is heavily dependent on precipitation. The mean annual precipitation for the Prairies ecozone is 454 mm, which is much less than the Canada-wide average of 535 mm (McGinn 2010). The spatial distribution of temperature over this ecozone is generally dominated by a latitude effect in the absence of any dramatic change in topography and mitigating impact of oceans (Bonsal et al. 2012). The average annual maximum and minimum temperature in this region are respectively 8.1 and −4.1 °C with considerable variability between seasons (McGinn 2010). Due to the high variability of precipitation in both time and space and relatively higher summer temperatures, this region is more susceptible to droughts (Pomeroy et al. 2011). Also, it has been found that circulation patterns in the upper atmosphere are associated with onset of droughts. Historically, this region was highly affected by many single- to multi-year droughts, including the most recent drought of 1999–2005.

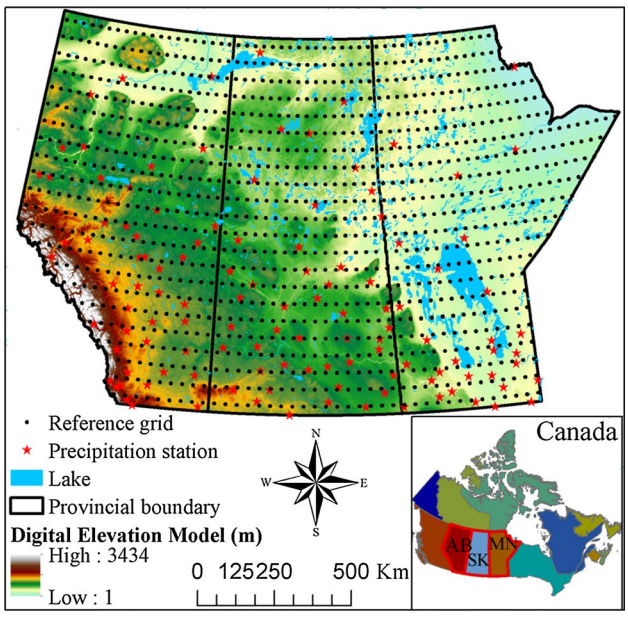

Fig. 1 Map of the study area overlaid with the reference grid; *inset* shows location of the study region (*AB* Alberta, *SK* Saskatchewan, *MN* Manitoba) in Canada

2.1 Observed data

Observed data used in this study consist of 10 km × 10 km gridded data of daily maximum and minimum temperatures (°C) and total daily precipitation (mm) for the 1961–2003 period. This dataset, available from Agriculture and Agri-Food Canada for the entire country south of sixty degrees north latitude, was interpolated from daily Environment Canada climate station observations using a thin-plate smoothing spline surface fitting method implemented by ANUsplin V4.3 (Hutchinson 2004). In the present study, this dataset is used for dividing the study area into smaller homogeneous regions to facilitate the development of uni- and multivariate frequency analysis approaches, to be discussed in the methodology section. In addition, a second set of station-based data consisting of daily precipitation and maximum and minimum temperatures, available from Environment Canada for the 1961–2003 period for a network of 120 stations located across the study area, is considered. This station-based dataset, which is commonly referred to as adjusted and rehabilitated dataset (Mekis and Vincent 2011), is used as an additional source for validating statistical homogeneity of regions identified on the basis of the gridded dataset discussed above. It is important to mention that some of the underlying stations are included in both datasets, but not necessarily the data itself due to incorporated adjustments in the second dataset.

2.2 Model simulations

Outputs from six different RCMs, driven by National Center for Environmental Prediction (NCEP) reanalysis II and four different Atmospheric-Ocean General Circulation Models (AOGCMs), available through NARCCAP are considered in this study (see Table 1). The aim of NARCCAP was to produce RCM simulations for a common period and domain (Mearns et al. 2009) to aid in systematic evaluation of various sources of uncertainty in future climate projections. These simulations were produced in two phases. In Phase I, simulations from CRCM, ECP2, HRM3, MM5I, RCM3 and WRFG RCMs were produced with boundary conditions from NCEP reanalysis II for a 25 year reference period (1981–2003). In Phase II, RCM simulations with boundary conditions taken from four different AOGCMs (i.e. CCSM, CGCM3, GFDL and HADCM3) for the 1970–1999 current and 2041–2070 future climates, with Special Report on Emissions Scenarios (SRES) A2 scenario (Nakicenovic et al. 2000), were produced. The NCEP-driven simulations are used to assess performance of individual

Table 1 The NARCCAP simulations used in the study

RCM	Driving AOGCM				Acronym for each model
	GFDL	CGCM3	HADCM3	CCSM	
CRCM	–	√	–	√	CRCM_CGCM3; CRCM_CCSM
ECP2	√	–	–	–	ECP2_GFDL
HRM3	√	–	√	–	HRM3_GFDL; HRM3_HADCM3
MM5I	–	–	√	√	MM5I_HADCM3; MM5I_CCSM
RCM3	√	√	–		RCM3_GFDL; RCM3_CGCM3
WRFG	–	√	–	√	WRFG_CGCM3; WRFG_CCSM

Details of RCMs and AOGCMS: *CRCM* Canadian Regional Climate Model (Caya and Laprise 1999), *ECP2* Experimental Climate Prediction (Juang et al. 1997), *HRM3* Hadley Regional Model 3 (Jones et al. 2003), *MM5I* NCAR Mesoscale Model (Grell et al. 1993), *RCM3* Regional Climate Model version 3 (Pal et al. 2007), *WRFG* Weather Research and Forecasting Grell Model (Grell and Devenyi 2002), *GFDL* Geophysical Fluid Dynamics Laboratory (GFDL GAMDT 2004), *CGCM3* Third General Coupled Global Climate Model (Flato 2005), *HADCM3* Hadley Centre Coupled Model version 3 (Gordon et al. 2000), *CCSM* Community Climate System Model (Collins et al. 2006)

RCMs, while 11 pairs of AOGCM-driven simulations for the current and future period are used in the assessment of projected changes to selected drought characteristics, discussed in the section on methodology. In this study, individual RCM simulations will be referred to as 'RCM_LBC', where RCM stands for the acronym of the RCM and LBC for the lateral boundary condition, i.e. NCEP reanalysis or the AOGCM driving the RCM at its boundaries. For example, CRCM simulation driven by CGCM3 will be referred to as CRCM_CGCM3. Though the simulation domains of the RCMs cover most of North America, as noted above, this study focuses only on Alberta, Saskatchewan and Manitoba provinces of Canada.

2.3 Reference grid

All RCMs have roughly the same horizontal resolution (i.e. 50-km) but different projections on the spherical earth. Therefore, a common reference grid (i.e. half-degree University of Delaware grid; Fig. 1) is considered in order to ease inter-comparison of results. All model outputs were interpolated to this reference grid using spline interpolation, while observed 10-km gridded data were aggregated to this reference grid before doing any analysis. This reference grid has been used in some previous studies wherein NARCCAP RCM simulations were used (e.g. Mearns et al. 2012).

3 Methodology

This section provides information on the framework used for deriving future changes to drought characteristics based on the NARCCAP multi-RCM simulations. It is important to note that most of the analyses are targeted at the level of individual grid cells which then feed into regional level analyses for the entire study area. Thus, first the procedures for deriving drought events are described, followed by identification of homogeneous regions of the study area and univariate and multivariate frameworks for frequency analysis of drought characteristics.

3.1 Drought indices, drought events and their characteristics

Various drought indices are available to detect and monitor droughts. However, the choice of indices depends mainly on the desired objectives of the study, available data, ease of computation, and interpretation of the results obtained. In this study, two different drought indices namely the SPI, which is solely based on precipitation, and SPEI, which is based on the difference between precipitation and potential evapotranspiration, are used to define drought events. By considering potential evapotranspiration, other meteorological variables such as temperature become relevant. According to Guttman (1998), the SPI, which is also recommended by WMO (2009), gives a better representation of drought-like conditions than the Palmer Drought Severity Index because it is the precipitation deficit that ultimately leads to hydrological and agricultural droughts. The SPEI has great potential to represent drought-like conditions as it considers a broader measure of the climatic water balance in the context of global warming compared to SPI (Potop et al. 2012; Jeong et al. 2014; Stagge et al. 2015). Both indices can be calculated for various time scales, e.g. 1-, 3-, 6-, 12-, 24-month etc., depending upon the nature of application. Based on the results reported in a related previous study (Masud et al. 2015), SPI and SPEI values corresponding to the 6-month time scale are used in this study. In the study of Masud et al. (2015), the 6-month time scale was found to capture well both short- and long-term meteorological droughts in the Saskatchewan River

Basin, which is the largest river basin of the study area. The calculation procedures of both SPI and SPEI are the same except the input variable. SPEI is calculated using the difference between precipitation and potential evapotranspiration (*PET*) (hereafter this difference is represented by *E*). Both simple and complex methods exist for calculating *PET*, however, the use of any method to calculate *PET* does not affect drought analysis much as noted by Mavromatis (2007). In this study, Hargreaves method (Hargreaves and Samani 1985), which simply uses the maximum and minimum temperature for estimating *PET*, is used. This method was ranked at the top among the temperature-based methods in the American Society of Civil Engineers Manual 70 analysis (Jensen et al. 1990). Wang et al. (2012) evaluated five temperature based approaches (i.e. Thornthwaite, Hargreaves, Linacre, Hamon and a vapor deficit method) to calculate monthly *PET* for Western North America and found Hargreaves method the best. Also, this method was recommended for estimating *PET* for the Canadian Prairies region in the inter-comparison study of Maulé et al. (2006). It is also important to note that Hargreaves and Samani (1982) and Mohan (1991) found that the Hargreaves method consistently produces accurate estimates of *PET* as compared to using the energy balance techniques, the Penman combination equation and the lysimetric methods.

Following a detailed comparative investigation based on the Kolmogorov–Smirnov (KS) and Z goodness-of-fit tests, the five parameter Wakeby distribution (Hosking and Wallis 1997; Masud et al. 2015) was selected to model *P* and *E* samples. The Wakeby distribution can mimic the shapes of many other commonly used skew distributions [e.g., Generalized Extreme Value (GEV), Generalized Normal (GNO), Pearson Type-III (PE3), Generalized Logistic (GLO), Generalized Pareto (GPA) etc.; Hosking and Wallis 1997] and therefore, has the potential to adapt to whichever distribution is suitable for a certain region/area/station. After estimating the distribution function of *P* and *E* samples at a six-month time scale for a given month, cumulative probabilities of *P* and *E* values are calculated. The SPI (SPEI) time series are produced by mapping the cumulative probabilities of *P* (*E*) series onto the standard normal distribution function for each case considered (i.e. observed and RCM_LBC cases). It is important to note that for calculating SPI and SPEI series for future climate, the cumulative probabilities of the future precipitation series are calculated from the fitted distribution functions for the current climate at the same grid cell of the same RCM_AOGCM simulation. To minimize the effect of minor droughts, drought events are identified considering a threshold of −0.50 for both SPI and SPEI, i.e., a drought event is considered when the value of SPI/SPEI is smaller than this threshold. Three important drought characteristics, i.e. duration (i.e. continuous sequence of SPI/SPEI values that satisfy the above threshold criterion), severity (i.e. cumulative sum of all SPI/SPEI values over the duration) and maximum severity (i.e. the largest drought severity within a drought event), are extracted for each drought event. However, for calculation convenience, drought severity is multiplied by −1. Some additional procedural details with schematic diagrams can be found in Masud et al. (2015).

3.2 Delineation of homogeneous geographic regions

The study area has been shown to be heterogeneous due to variations in climatic patterns and topographic features (Armstrong et al. 2015) and, therefore, is divided into smaller statistical homogeneous regions using cluster analysis, which is one of the commonly used statistical multivariate analysis techniques. Individual grid characteristics, i.e. geographic location (latitude, longitude and elevation), average drought severity and duration and mean annual precipitation are used as input attributes. Using this technique, one combines a set of sites (i.e. grid locations in the present study) into groups with similar characteristics or features of interest (Hosking and Wallis 1997; Rao and Srinivas 2008). Herein, hierarchical clustering (Kaufman and Rousseuw 1990) is used for the entire study area. This technique cannot always provide exact formation of groups and, therefore, some subjective adjustments are applied in order to arrive at meaningful contiguous geographic regions (Hosking and Wallis 1997; Masud et al. 2015). Once such regions are delineated, their statistical homogeneity needs to be tested. For this purpose, Hosking and Wallis (1997) proposed an L-moments-based univariate test. According to this test, statistics of only one drought characteristic (e.g. either drought severity or drought duration) can be considered. The regions found homogeneous on the basis of the univariate test may not always be homogeneous for different drought characteristics in a multivariate context. This problem is resolved by using multivariate L-moments-based multivariate homogeneity tests of Chebana and Ouarda (2007). Multivariate L-moments were developed by Serfling and Xiao (2007). It is important to note that a homogeneous region helps to increase the effective length of data, which in turn increases the accuracy of the estimated return levels.

3.3 Regional characteristics of drought severity and duration

After verifying statistical homogeneity of all delineated regions based on uni- and multivariate approaches discussed above, the next step is to select a flexible regional distribution for each homogeneous region from some suitable candidate distributions in order to develop regional growth curves. A regional growth curve represents a

dimensionless relationship between frequency and magnitude of the selected drought characteristic. The distributions considered in this study include GEV, GLO, GPA, PE3, GNO, and Wakeby. These distributions are commonly used for frequency analysis of hydro-climatic extremes. Based on the Z and KS tests, multiple candidates (i.e. PE3, GPA and Wakeby) are found suitable for most of the regions. It is important to mention that the distribution of thresholded samples asymptotically converges to the GPA distribution (Coles 2001). Based on this theoretical reasoning and the empirical support from the Z and KS tests, the GPA distribution is selected for modeling regional growth curves of selected characteristics of observed drought events. The same distribution is used to model growth curves of RCM_NCEP as well as current and future period RCM_AOGCM simulated characteristics of drought events, however, with parameters re-estimated for each case considered.

Observed regional 20- and 50-year return levels of drought characteristics for each homogeneous region are computed by multiplying regional growth factors, derived from respective regional growth curves with the respective regionally-averaged grid-cell based mean values of drought characteristics. When deriving growth factors, the impact of rate of annual exceedances is taken into account using regionally-averaged grid-cell based values of rate of exceedances (i.e. the number of extreme values per year). Exactly, the same procedure is used for RCM_AOGCM current and future period simulations.

3.4 Copula-based bi- and trivariate analyses

The copula is a multivariate distribution function with all the univariate marginal distributions being uniform on the interval [0, 1]. Based on Sklar's (1959) theorem, the joint cumulative distribution function of two or more correlated variables can be expressed as:

$$H(x_1, x_2, \ldots, x_n) = C[F_1(x_1), F_2(x_2), \ldots, F_n(x_n)] \tag{1}$$

where $x_1, x_2, \ldots, x_n$ are random variables with marginal distributions, $F_1(x_1), F_2(x_2), \ldots, F_n(x_n)$, and C is the copula function. The n-dimensional Archimedean copula (Nelsen 2006) can be expressed as:

$$C^n(u) = \varphi^{[-1]}(\varphi(u_1) + \varphi(u_2) + \cdots + \varphi(u_n)) \tag{2}$$

where the superscript on C denotes dimension; $u_i = F_i(X_i)$ is the marginal cumulative distribution function (cdf) of variable $X_i (i = 1, 2, 3, \ldots, n)$; $\varphi(.)$ = copula generator which needs to be completely monotonic and φ^{-1} is the pseudo inverse of $\varphi(.)$. For the trivariate case, a fully nested Archimedean copula is constructed by nesting symmetric copulas (Embrechets et al. 2003; Savu and Trede 2010; Wong et al. 2010):

$$\begin{aligned} C(u_1, u_2, u_3) &= C_1\left[C_2(u_1, u_2), u_3\right] \\ &= \varphi_1^{-1}\left(\varphi_1\left\{\varphi_2^{-1}\left[\varphi_2(u_1) + \varphi_2(u_2)\right] + \varphi_1(u_3)\right\}\right) \end{aligned} \tag{3}$$

where C_1 and C_2 are two bivariate one-parameter copulas; C_2 is the copula describing the dependence between variables u_1 and u_2 and the outer copula C_1 is a function of the inner copula and u_3.

The Gumbel–Hougaard (GH) copula is a common choice for many hydro-climatic applications, because it includes multivariate extreme distributions which exhibit tail dependence and has been found to provide reasonable fit to field data (Nelsen 2006; Serinaldi and Grimaldi 2007; Wong et al. 2010). The GH copula with two- and three-variable versions is given by:

$$C(u_1, u_2) = \exp\left\{-\left[(-\ln u_1)^{\theta} + (-\ln u_2)^{\theta}\right]^{1/\theta}\right\}, \quad \text{and} \tag{4}$$

$$\begin{aligned} &C_1\left[C_2(u_1, u_2), u_3\right] \\ &= \exp\left\{-\left(\left[(-\ln u_1)^{\theta_2} + (-\ln u_2)^{\theta_2}\right]^{\theta_1/\theta_2} + (-\ln u_3)^{\theta_1}\right)^{1/\theta_1}\right\} \\ &\theta_1 < \theta_2, \theta \in (1, \infty) \end{aligned} \tag{5}$$

To evaluate the fitted copula, the procedure proposed by Genest et al. (2009) is used.

3.5 Estimation of drought risks

In this study, first the joint occurrence probabilities of drought severity S and duration D are considered, i.e. drought severity and duration both exceed a certain threshold value at the same time (i.e. $S > s$ and $D > d$). Corresponding relationships of the joint occurrence probabilities are given below:

$$\begin{aligned} P_1 &= P(S > s \text{ and } D > d) = P(S > s \cap D > d) \\ &= 1 - F_S(s) - F_D(d) + C\{F_S(s), F_D(d)\} \end{aligned} \tag{6}$$

Similar relationships can be developed for "duration and max severity" and "severity and maximum severity" pairs. All three types of joint bivariate occurrence probabilities are evaluated in order to identify drought sensitive regions.

Similarly, trivariate joint occurrence probabilities of drought severity, duration and maximum severity are also evaluated, i.e. drought severity and duration and maximum severity exceeding respective specific thresholds at the same time (i.e. $S > s$ and $D > d$ and $S_{\max} > s_{\max}$). Here, s, d and $s_{\max}$ denote the severity, duration and maximum severity values corresponding to selected 20-, and 50-year return periods. The joint occurrence probability is given by:

$$
\begin{aligned}
P_2 &= P(S > s \text{ and } D > d \text{ and } S_{\max} > s_{\max}) \\
&= P(S > s \cap D > d \cap S_{\max} > s_{\max}) \\
&= 1 - F_S(s) - F_D(d) - F_{S_{\max}}(s_{\max}) \\
&\quad + C\{F_S(s), F_D(d)\} + C\left\{F_S(s), F_{S_{\max}}(s_{\max})\right\} \\
&\quad + C\left\{F_D(d), F_{S_{\max}}(s_{\max})\right\} \\
&\quad - C\left\{F_S(s), F_D(d), F_{S_{\max}}(s_{\max})\right\} \qquad (7)
\end{aligned}
$$

Based on the results of the KS test and theoretical reasons behind thresholded samples (Coles 2001), the GPA distribution is selected to model drought severity, drought duration, and maximum severity.

4 Results and discussion

In this section, identification of statistical homogeneous regions is presented first, followed by other important analyses including validation of RCMs, impact of driving fields, projected changes to drought characteristics, and identification of drought sensitive regions. Analysis of drought severity and duration provide similar results and, therefore, detailed results are presented for drought severity and only selected results for drought duration. For the validation of RCM simulated drought characteristics, we first describe the behavior of ensemble-averaged values and then the performance of individual models. For the analysis of future droughts, detailed assessment is presented and discussed. Statistical significance of projected changes is assessed following a bootstrapped based non-parametric test (Efron and Tibshirani 1993; Mladjic et al. 2011) at the 5 % significance level for both SPI and SPEI cases. However, the results are discussed mainly for the SPEI case.

4.1 Geographic homogeneous regions

Based on the behavior of drought characteristics and geographic location attributes, the study area is divided into 15 regions/partitions (i.e. Region 1 to 15) using hierarchical clustering (Fig. 2). It is important to mention that Region 9 is divided further into three parts (a western, 9 W, and an eastern, 9E, part and Region 11) based on various trials of hierarchical clustering in order to ensure greater homogeneity. Both the western and eastern parts are referred together as one region. The results of univariate analysis for drought severity suggest that most of the regions could be considered homogeneous or acceptably homogeneous, except Region 1 and 15. A few regions are found non-homogeneous (i.e. Region 2, 4, and 13) for drought duration. However, based on the results of the bivariate homogeneity test of drought severity and duration together, all regions are found homogeneous. Furthermore, in addition to the drought characteristics derived from observed 10-km gridded data, homogeneity of all 15 regions is also tested using drought characteristics derived from station-based adjusted and rehabilitated data available from 120 stations for the 1961–2003 period. Results from this validation also reveal that all regions could be considered homogeneous based on drought severity. Similar results are noted for drought duration for most of the regions, except two (Region 1 and 2), which are found to be within an acceptably homogeneous category. On the basis of this station-based dataset, results of bivariate homogeneity testing also suggest that all regions could be considered homogeneous. In addition to the above presented validations, homogeneity of the identified regions is also tested using drought characteristics derived from observed 50-km resolution gridded data and NCEP-driven RCM simulated data. For these cases, similar results are found as noted above. Validation of homogeneous regions using drought characteristics derived from multiple datasets originating from different sources provides a sound basis to develop additional analyses based on these regions.

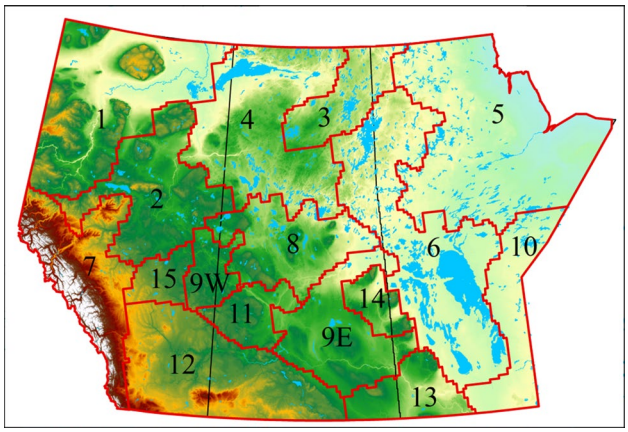

Fig. 2 Fifteen homogeneous regions (Region *1* to *15*) delineated on the basis of hierarchical clustering of drought characteristics and geographic location attributes and verified using the uni- and multivariate homogeneity analysis approaches

4.2 Validation of RCM-simulated drought characteristics and lateral boundary forcing errors

First, spatial patterns of observed values of mean drought severity, shown in Fig. 3a, are discussed before validation of RCMs. From this figure, it can be noticed that three southern regions (i.e. Region 11, 12 and 15) and three northwestern regions (i.e. Region 1, 2 and 4) are associated with larger values of drought severity compared to the other regions—meaning that these regions appear to be relatively more drought prone. RCM-simulated ensemble-averaged mean drought severity is shown in Fig. 3b and the

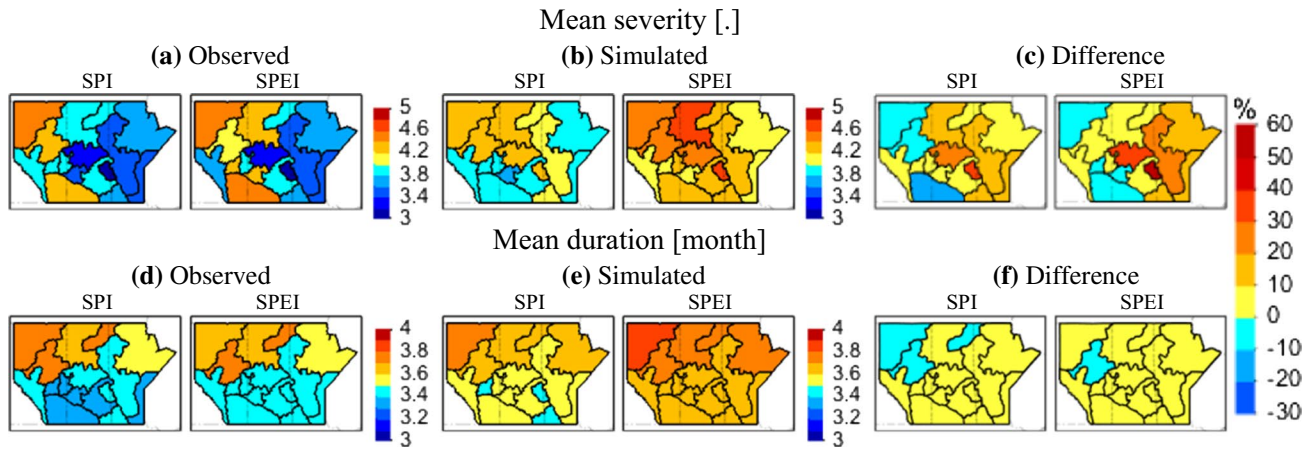

Fig. 3 Comparison of observed and ensemble averaged RCM_NCEP simulated mean drought **a**, **b** severity and **d**, **e** duration for the 1981–2003 period. Relative differences (normalized with the observed values) between results shown in **b**, **a** and **e**, **d** panels are given in **c** and **f**, respectively

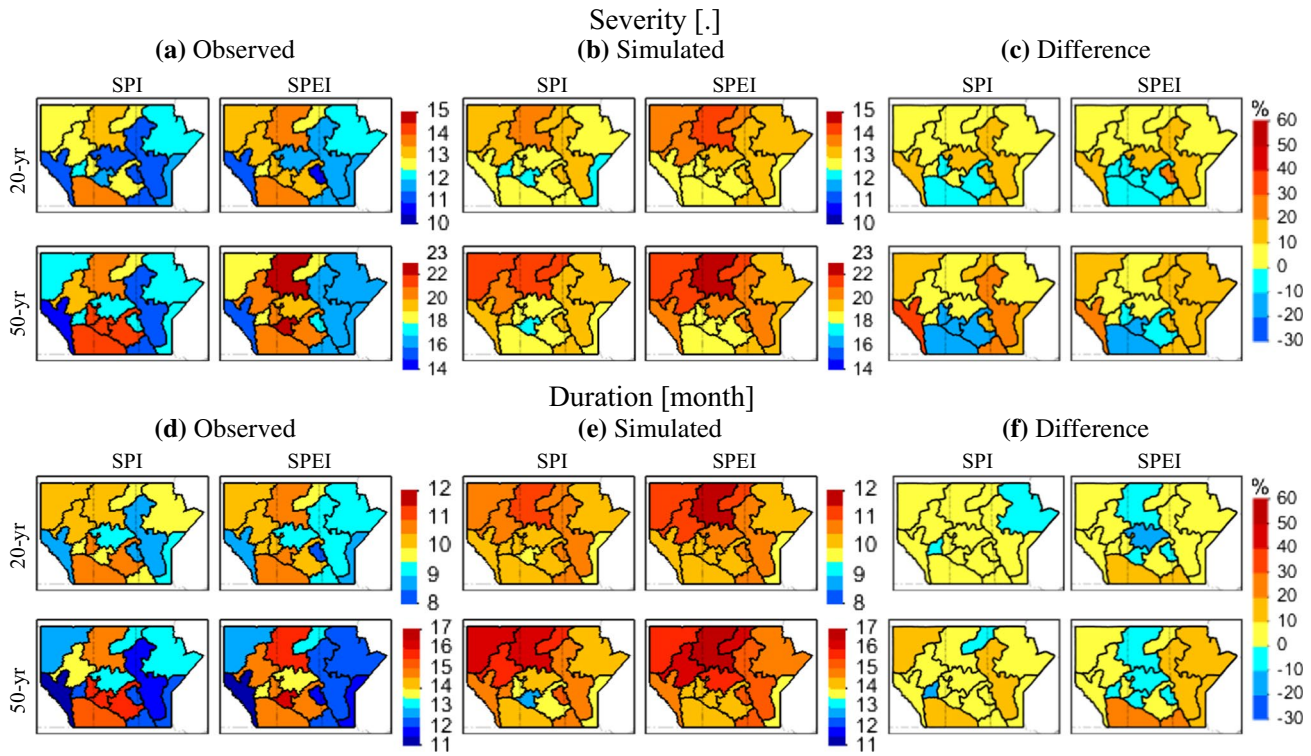

Fig. 4 Comparison of observed and ensemble averaged RCM_NCEP simulated 20- and 50-year regional return levels of drought **a**, **b** severity and **d**, **e** duration for the 1981–2003 period. Relative differences (normalized with the observed values) between return levels shown in **b**, **a** and **e**, **d** are given in **c** and **f**, respectively

relative differences from the corresponding observed values in Fig. 3c. In general, ensemble-averaged drought severity for both SPI and SPEI cases differ from that obtained from observed data for various regions. RCMs tend to produce relatively more severe droughts for central and eastern regions. Typical differences lie within the −20 to 50 % range. Similar spatial patterns are found for mean values of drought duration for various regions (Fig. 3d, e), however, with differences lying typically within the ±10 % range (Fig. 3f).

The spatial patterns of observed and NCEP-driven RCM simulated regional return levels of drought severity are

shown in Fig. 4. Figure 4a shows that the spatial patterns of observed return levels are very similar to those of mean severity shown in Fig. 3a. Overall, smaller return levels are found for many eastern and a few south-western regions (e.g. Region 7). The performance errors of all RCMs are assessed by comparing regional return levels of drought severity derived from NCEP-driven RCM simulations to those derived from observed gridded data. Ensemble-averaged regional return levels of drought severity are shown in Fig. 4b and their relative differences from the corresponding observed values in Fig. 4c. Like mean severity, ensemble-averaged return levels for both SPI and SPEI cases differ from those obtained from observed data for various regions. In general, RCMs tend to produce more severe droughts for many northern and eastern regions. Typical differences lie within −20 to 40 % range, with the southern part of the study area (Region 9, 11, 12 and 15) associated with negative differences and other regions associated with positive differences. Overall, relative differences (i.e. performance errors) are larger for the 50-year return level compared to the 20-year return level. For return levels of drought duration, results are similar to those of severity except that the magnitude of over-/underestimation is relatively smaller.

Now we turn to the performance of individual models. Figure 5 shows relative differences between 20- and 50-year regional return levels of drought severity derived from NCEP-driven RCM simulations and observed data (Fig. 4a) for each of the six RCMs separately. For the 20-year return levels, the relative differences lie between ±10 % for most of the regions and RCMs except HRM3 which overestimates (up to 60 %) for some eastern regions. The results for the 50-year return levels are similar to those for the 20-year return levels, but with a wider range of relative differences (−30 to 60 %). For western regions (Region 1 and 7), all six RCMs overestimate 50-year return levels. For eastern regions (i.e. Region 5, 6 and 10), four of the six RCMs (i.e. HRM3, MM5I, RCM3 and WRFG) overestimate 50-year return levels, while the other two (i.e. CRCM and ECP2) exhibit a mixed behavior. Like the 20-year return level, HRM3 overestimates 50-year return level by up to 60 % for many regions. Most of the RCMs underestimate 50-year return levels for southern regions (i.e. Region 9, 11 and 12) and overestimate it for Region 13. In general, ensemble-averaged positive or negative relative differences shown in Fig. 4c are smaller than those noted for individual RCMs and lie within a smaller range (i.e. −20 to 40 %) for the majority of the regions. The relative differences between 20- and 50-year regional return levels of drought duration derived from NCEP-driven RCM simulations and observed data (given in Fig. 4d) are shown in Fig. 6 separately for each of the six RCMs. Here, the spatial patterns are very close to the pattern of regional return levels of drought severity. The physical reasons for this over- or underestimation by an individual RCM outcome may depend on model formulation and

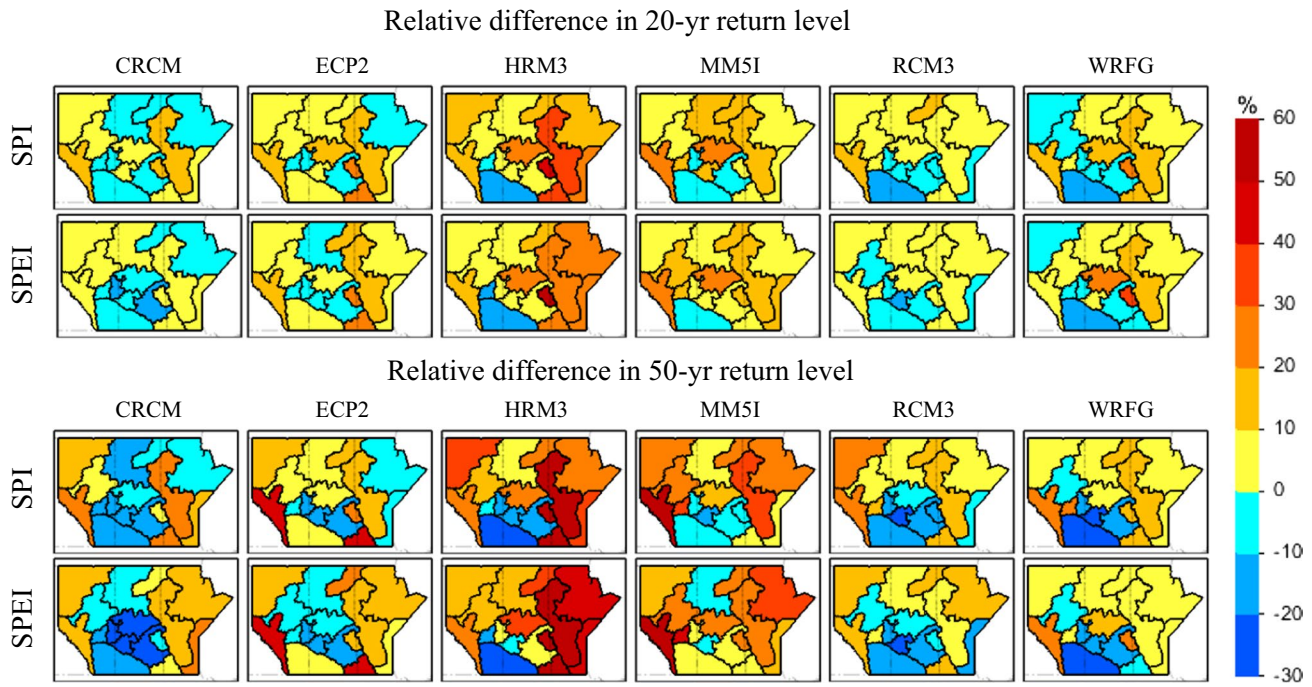

Fig. 5 Relative difference (in %) between observed and RCM_NCEP simulated 20- and 50-year regional return levels of drought severity for the 1981–2003 period. The differences are normalised with the observed values

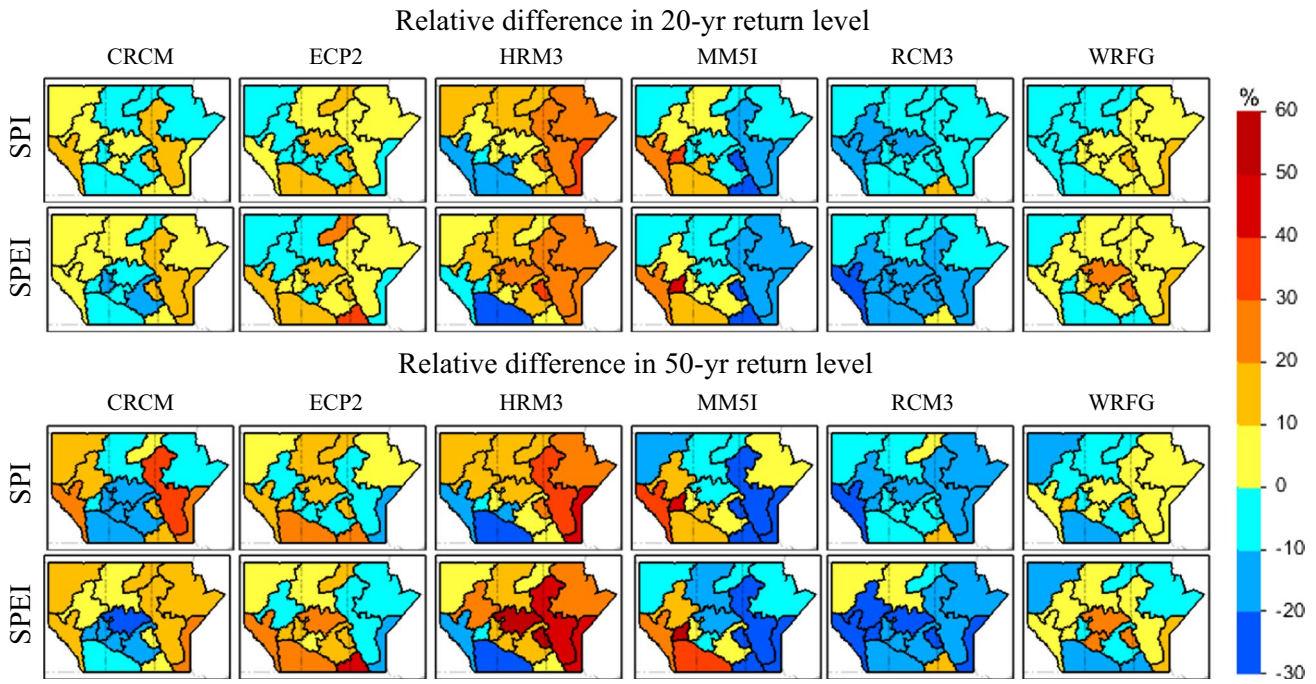

Fig. 6 Relative difference (in %) between observed and RCM_NCEP simulated 20- and 50-year regional return levels of drought duration for the 1981–2003 period. The differences are normalised with the observed values

parameterization schemes of the respective RCM. These models have variations in the physical parametrizations, especially in the parameterized sub-grid scale processes which include sub-grid scale turbulence, radiative transport, boundary layer effects and moist processes. The moist processes include parameterized treatments of shallow and deep convective cloud processes as well as larger scale cloud physics (Mearns et al. 2012; Wehner 2013). In addition, the specifications of the surface and soil properties implemented in the land surface schemes of RCMs and the degree and sophistication of various land–atmosphere feedback mechanisms could also play a role.

The impact of the driving fields (i.e. the lateral boundary forcing errors) is assessed by comparing NCEP- and AOGCM-driven simulations for the 1981–2000 period. A comparison of 20- and 50-year return levels of SPI- and SPEI-based severity and duration is illustrated in Fig. 7. Five out of six RCMs were driven by two different AOGCMs, while another one was driven by only one AOGCM, leading to the eleven sets of scatterplots for both SPI and SPEI cases, shown in Fig. 7. It should be noted that for both severity and duration, the difference between AOGCM- and NCEP-driven RCM simulated 20-year return levels are smaller than those for the 50-year return levels. More specifically, for example, 50-year return levels for AOGCM-driven simulations are smaller than those for NCEP-driven simulations for HRM3, while for WRFG, return levels for AOGCM-driven simulations are larger than those of NCEP-driven simulations for the majority of the regions. For both HRM3 and WRFG, the lateral boundary forcing errors are slightly larger in the case of SPEI-based severity and duration than that of SPI-based severity and duration. Overall, the average boundary forcing errors are less than 10 % for the majority of the cases and larger differences are associated with longer return periods, in general. Comparison of RCM performance errors and boundary forcing errors show that performance errors are larger than the boundary forcing errors for most of the cases.

4.3 Projected changes to drought characteristics

Figure 8a provides projected changes to SPI and SPEI based mean severity for the 2041–2070 period relative to 1970–1999 for individual RCM_AOGCM pairs. These changes, projected by the majority of the RCM_AOGCM pairs (eight out of eleven), are mostly positive for southern parts of the study area. It can be noticed from the results of SPEI-based analysis that completely positive changes are projected by three out of eleven simulation pairs (CRCM_CCSM, HRM3_HADCM3 and MM5I_HADCM3) for all regions, while the rest of the simulation pairs project a decrease in drought severity specifically for regions located in the northern parts of the study area. Similar spatial patterns are found for mean drought duration (see Fig. 8b), but changes are of relatively smaller magnitude for most of the regions. Overall, SPEI based ensemble-averaged

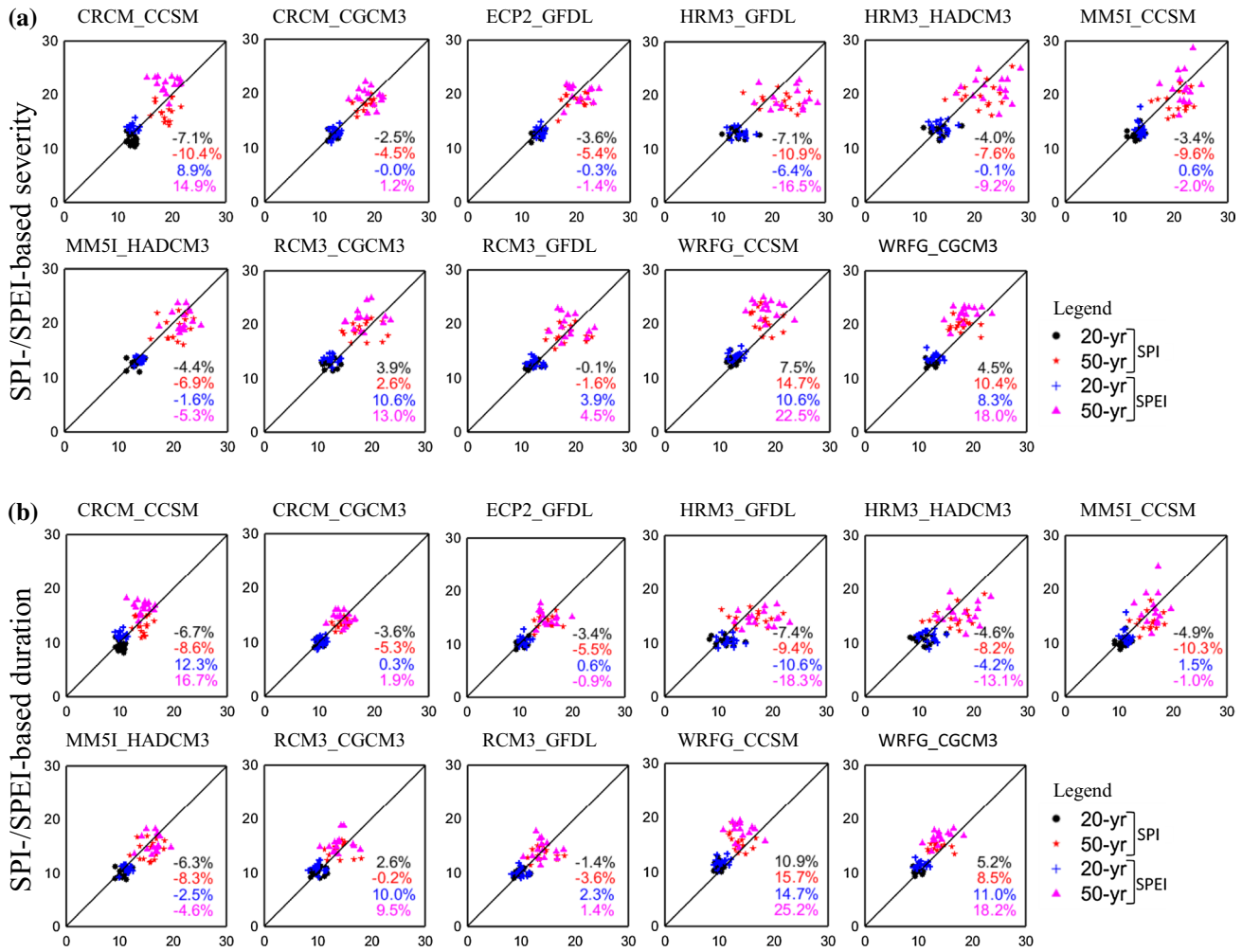

Fig. 7 Scatterplots of 20- and 50-year regional return levels of SPI- and SPEI-based **a** severity and **b** duration for the 1981–2000 period. The x-axis corresponds to NCEP driven RCM simulation, while the y-axis corresponds to AOGCM driven simulation. *Numbers in each panel* represent average percentage difference between the AOGCM- and NCEP-driven simulated return levels (normalized with the latter). Results based on SPI are shown in *black* and *red color* and those for the case of SPEI are shown in *blue* and *pink color*

projected changes shown in Fig. 8 indicate increases in both drought severity and duration in southern parts of the study area, with more pronounced changes in mean severity. With respect to statistical significance of projected changes, based on the nonparametric bootstrap test, from four to eight (out of eleven) RCM_AOGCM pairs suggest significant positive changes to mean severity and duration for most of the regions (e.g. Region 9, 11, 12, 13 and 15) in southern parts and significant negative changes for most of the regions (e.g. Region 1, 3, 4 and 5) in northern parts of the study area.

The effect of temperature on defining drought characteristics is visible in SPEI-based results of all RCM_AOGCM pairs. The spatial patterns of mean annual precipitation suggest an increase in precipitation over the study area (see "supplemental material"). However, at the same time, mean annual *PET* has been projected to increase for most of the RCM_AOGCM combinations possibly due to the projected increase in the mean annual temperature in the 1 to 3 °C range. Thus, the projections of the underlying variables (i.e. *P*, *T* and *PET*) used for calculating drought indices generally support the changes noted in drought characteristics in the future over the study area. It is important to note that an analysis on the annual basis is just a simple way of uncovering the impact of underlying variables on changes to drought characteristics.

Projected changes to drought severity at the regional level are also studied by comparing 20- and 50-year return levels derived from AOGCM-driven RCM simulations for the future 2041–2070 period with those for the current 1970–1999 period. Figure 9a, b shows percentage changes to 20-year return levels of drought severity and duration at the regional scale. It is noteworthy to mention

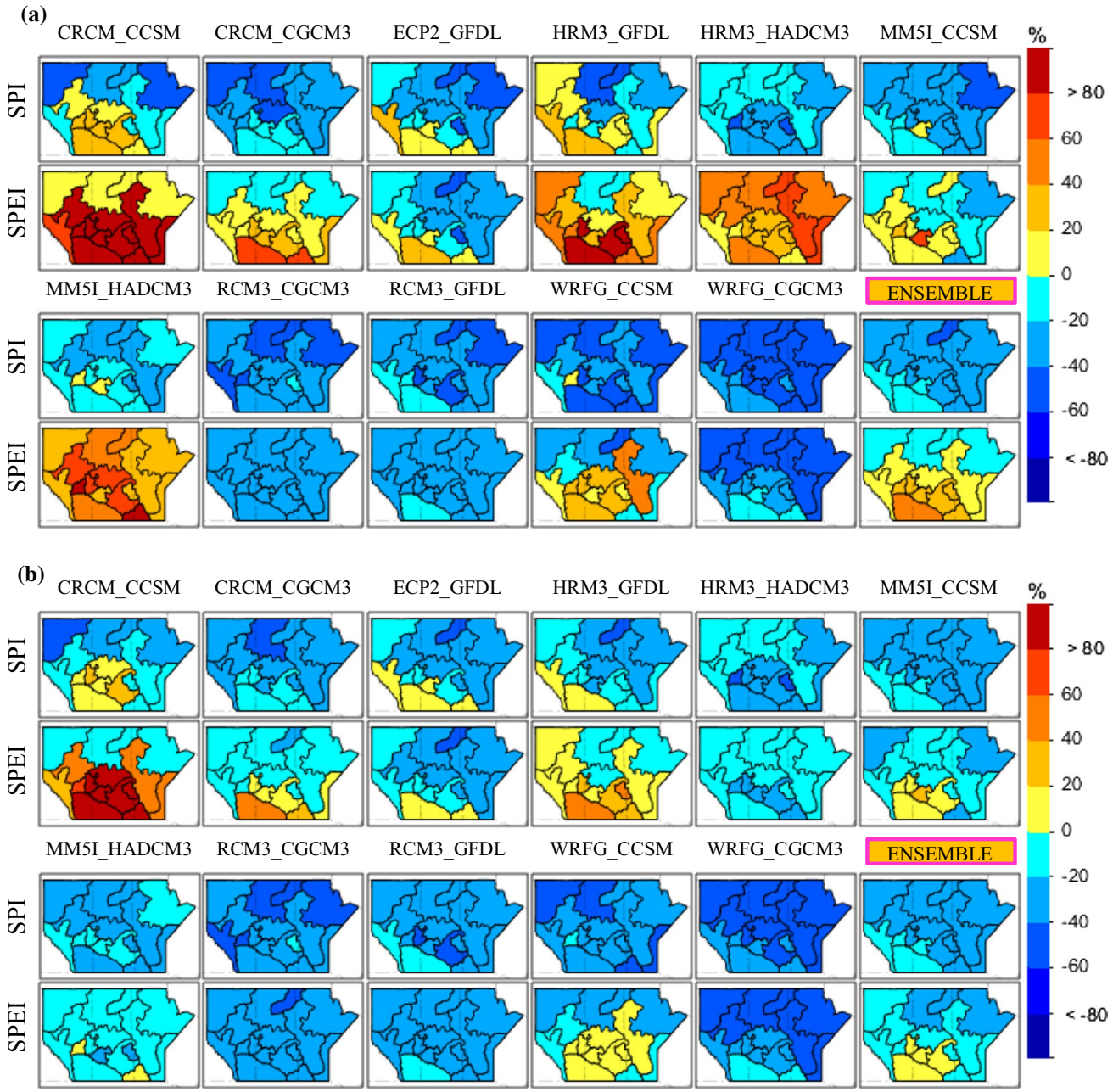

Fig. 8 Projected changes (in %) to SPI and SPEI based **a** mean drought severity **b** mean drought duration for the 2041–2070 period with respect to the current 1970–1999 period

that the spatial patterns are somewhat similar to the spatial patterns found for drought severity and duration in Fig. 8. For the case of 50-year return levels, this behavior of AOGCM-driven RCM simulations stays about the same (see Fig. 10). The magnitude of projected changes in 50-year return levels is relatively smaller than that in the 20-year return levels. Average projected change for all RCM_AOGCM pairs shows that the 20-year return level will increase by up to 60 % for drought severity and 40 % for drought duration in southern regions, while 50-year return level will increase by up to 40 % for drought severity and 20 % for drought duration in the same parts of the study area. Following the bootstrap based nonparametric test, positive projected changes to 20- and 50-year regional return levels are found statistically significant for most of the RCM_AOGCM combinations for some southern regions (e.g. Region 12, 13 and 15) and negative changes are found significant for most of the northern regions (e.g. Region 1, 3, 4 and 5). In general, the number of RCM_AOGCM pairs that suggest significant changes is smaller

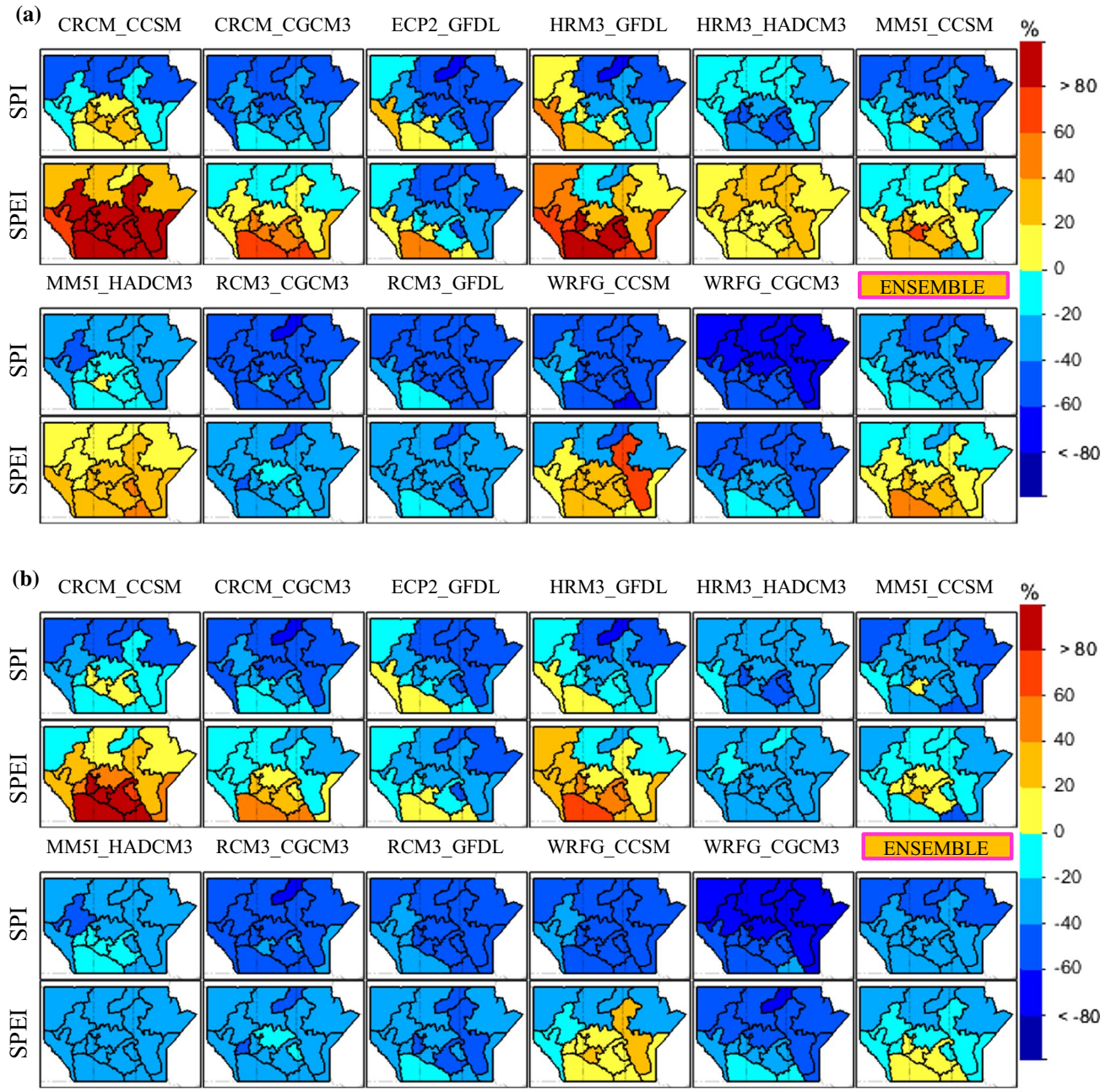

Fig. 9 Projected changes (in %) to regional 20-year return levels of drought **a** severity and **b** duration for the 2041–2070 period with respect to the current 1970–1999 period

for longer return periods (e.g. 50-year), especially for the southern regions.

A comparison of analyses shown in Figs. 9 and 10 suggests considerable influence of the driving AOGCM on the magnitude and sign of the projected change. For example, results based on CRCM_CCSM suggest considerably larger increases compared to CRCM_CGCM3. Therefore, the use of multiple AOGCMs at the RCM boundaries is important for addressing uncertainties associated with the driving fields. Considerable variation in the results has also been noticed across different RCMs, which are forced by the same AOGCM. For example, the results based on ECP2_GFDL suggest smaller increases compared to HRM3_GFDL. As mentioned before, the variation in the results of different RCMs may depend on the model formulation and parameterization schemes of the respective RCM, although they are governed by the same AOGCM at the boundaries.

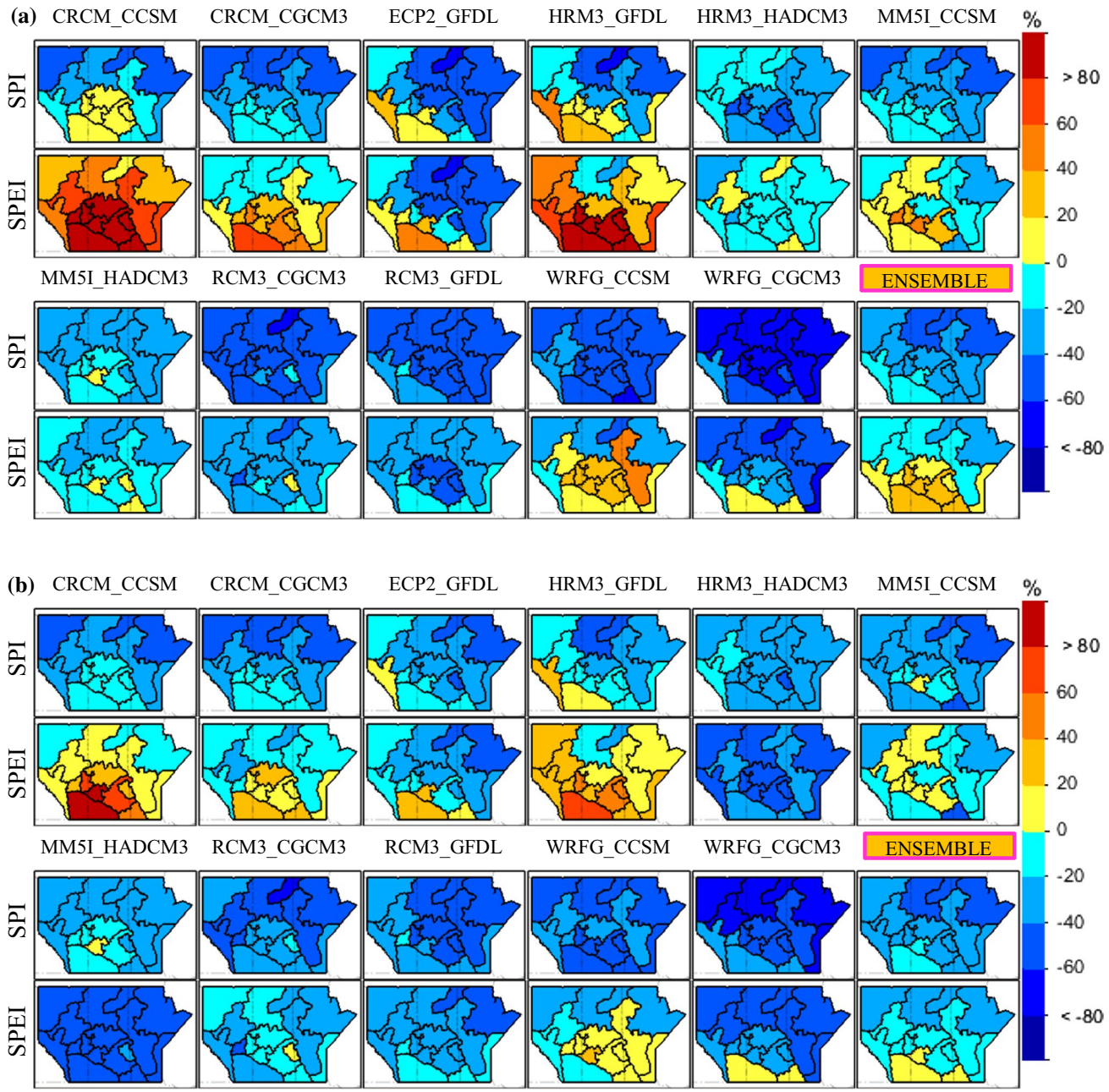

Fig. 10 Projected changes (in %) to regional 50-year return levels of drought **a** severity and **b** duration for the 2041–2070 period with respect to the current 1970–1999 period

4.4 Drought vulnerable regions

As the drought characteristics are highly correlated, multivariate analysis using copulas seems important for evaluating drought risks across the study area. Therefore, two joint occurrence probabilities are considered in this study for the current and future periods as described in Sect. 3.5, i.e. $P_1 = P(S > s \text{ and } D > d)$ and $P_2 = P(S > s \text{ and } D > d \text{ and } S_{\max} > s_{\max})$. In this study, the thresholds s, d and $s_{\max}$ correspond to 20- and 50-year return values obtained from univariate analyses. Figure 11 shows percentage changes in (a) bivariate and (b) trivariate probabilities for the case of 20-year return period threshold. A discernible spatial pattern of drought sensitive regions is visible in this figure, which is consistent with the findings discussed in the previous section that southern regions are more susceptible to droughts in the future compared to the northern regions. Based on bivariate analyses, seven out of eleven RCM_AOGCM pairs indicate that southern regions are associated with higher

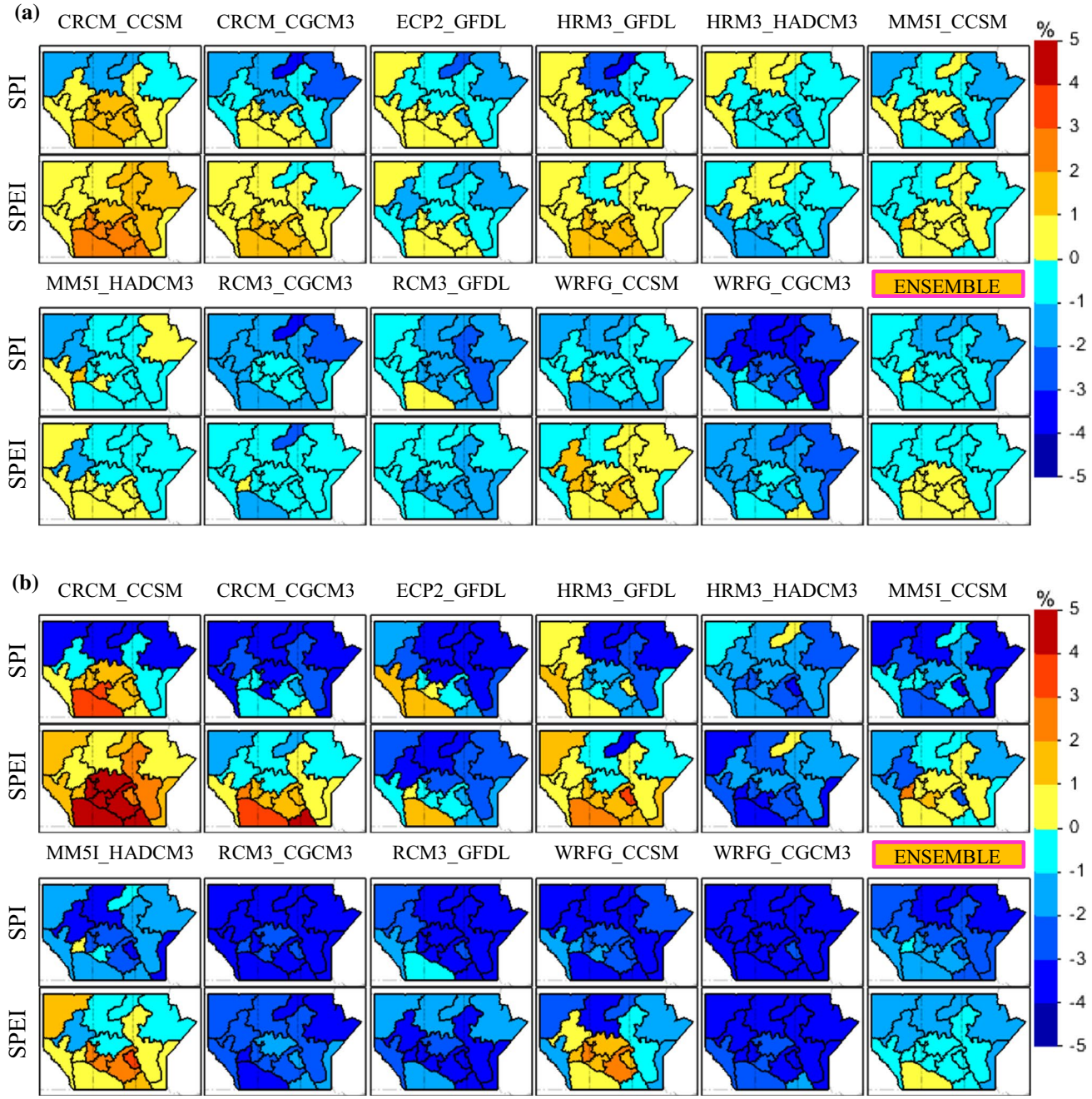

Fig. 11 Changes (in %) to **a** bivariate joint occurrence probabilities corresponding to 20-year return period thresholds of S and D and **b** trivariate joint occurrence probabilities corresponding to 20-year return period thresholds of S, D and S_{max} for the 2041–2070 period with respect to the current 1970–1999 period

drought risks in the future. Similar analyses are also performed for other bivariate cases (i.e. severity and maximum severity; duration and maximum severity). Their results (not shown) broadly suggest similar patterns. Southern regions remain susceptible to droughts when trivariate joint occurrence probabilities are considered, while northern regions become less susceptible (Fig. 11b). Consequently, the impact of considering three instead of two drought characteristics for identifying drought sensitive regions is obvious.

Figure 12 shows percentage changes in (a) bivariate and (b) trivariate probabilities for the case of 50-year return period thresholds. For this case, almost analogous spatial patterns of drought sensitive regions are found. It is interesting to note that, compared to other RCM_AOGCM pairs, only CRCM_CCSM produces highly positive changes in joint

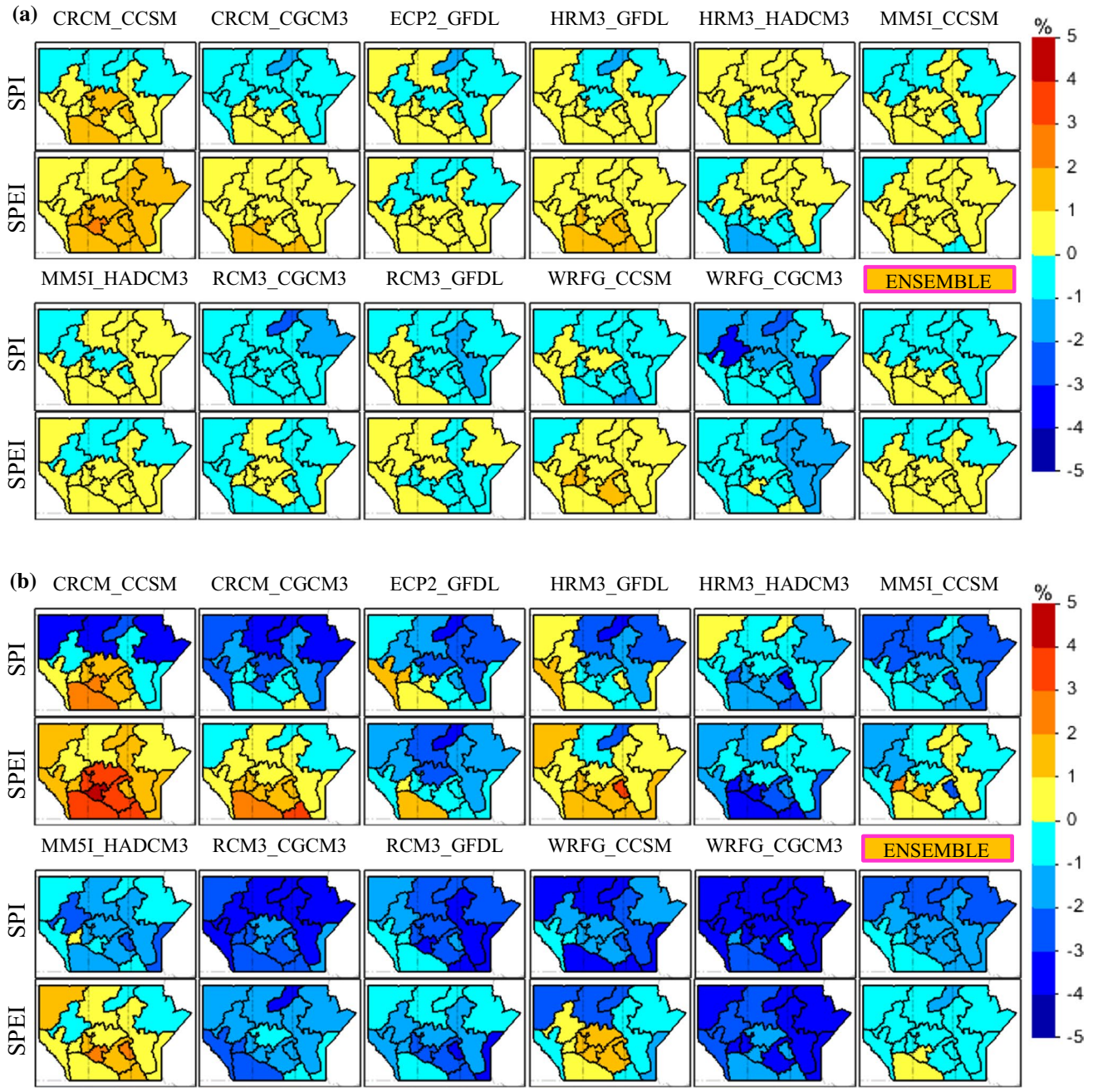

Fig. 12 Changes (in %) to **a** bivariate joint occurrence probabilities corresponding to 50-year return period thresholds of S and D and **b** trivariate joint occurrence probabilities corresponding to 50-year return period thresholds of S, D and S_{max} for the 2041–2070 period with respect to the current 1970–1999 period

occurrence probabilities for both bi- and trivariate cases. Overall, ensemble-averaged projected changes for the case of 20-year return period threshold show higher drought risks for central and southern parts of the study area (i.e. Region 8, 9, 11, 12, 13, and 14 for the bivariate case and Region 12 for the trivariate case). The pattern of drought sensitive regions for the 50-year return period threshold case are almost identical to the 20-year case, however, with few additional regions in the western and eastern parts of the study area (Region 2, 6, 7 and 10 for the bivariate case and Region 11 for the trivariate case) are identified as vulnerable. The statistical significance of percentage changes in joint probabilities corresponding to 20- and 50-year return period threshold is assessed at the 5 % significance level using the two-sample Wilcoxon rank-sum test (Walpole et al. 2012). The majority of the RCM_AOGCM pairs suggest significant positive

changes for most of the southern regions (e.g. Regions 9, 11, 12, 13 and 15) and significant negative changes for some of the northern regions (e.g. Regions 1, 4 and 5).

4.5 Drought analysis for the agricultural growing season

Finally to complete the analysis, we evaluate projected changes to drought characteristics specifically for the agricultural growing season (May–August) due to the fact that southern parts of the study area support a vibrant agro-based economy, which was impacted negatively due to many historical droughts. During the growing season, the study area receives the majority of the annual precipitation and also observes higher seasonal temperatures and hence occurrence of drought like conditions can have severe impacts on the agriculture sector. For this analysis, drought indices (SPI and SPEI) and drought characteristics are determined separately for the growing season. Projected changes to mean drought severity and duration are shown

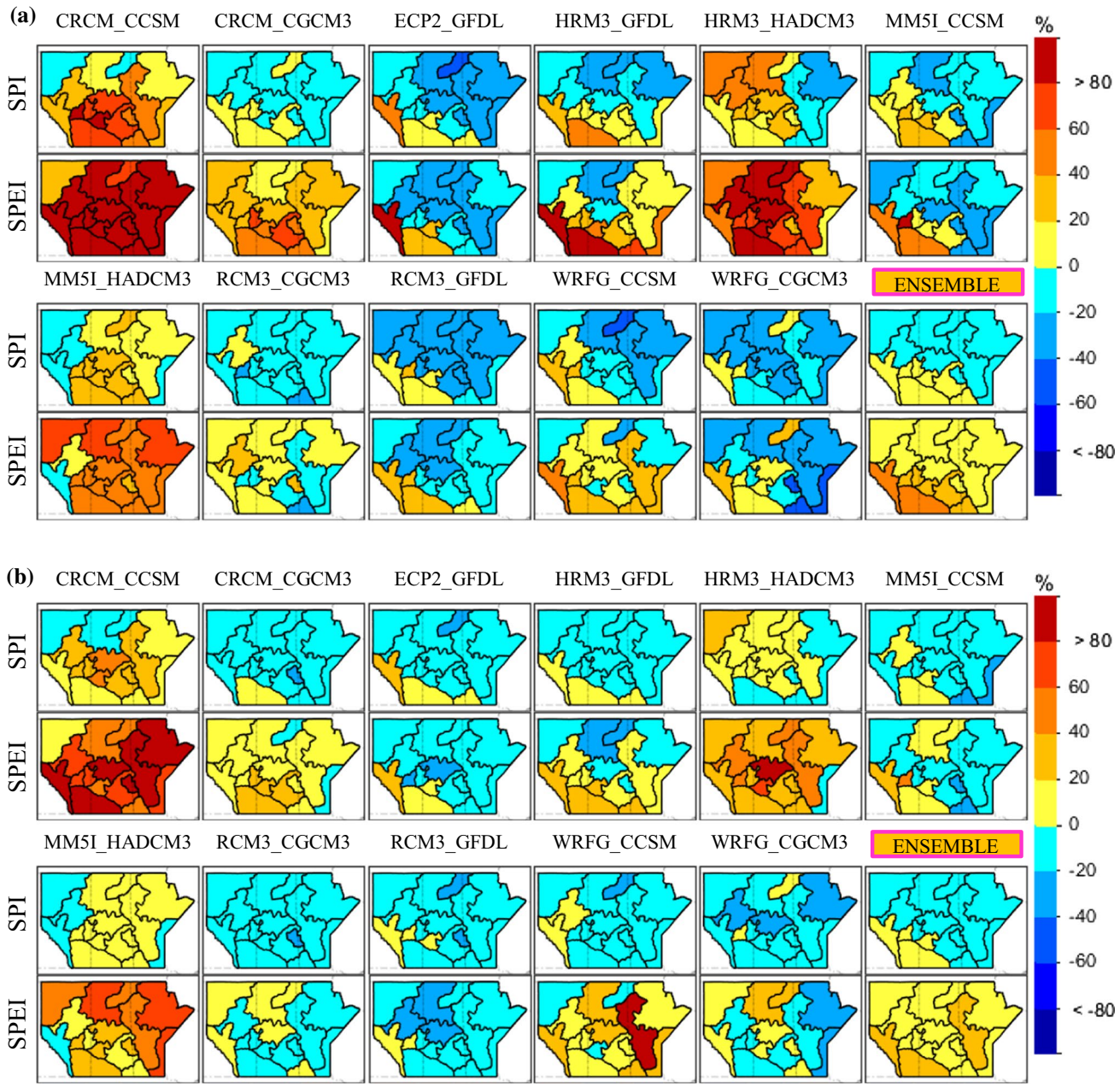

Fig. 13 Projected changes (in %) to SPI- and SPEI-based **a** mean drought severity **b** mean drought duration for the 2041–2070 period with respect to the current 1970–1999 period for the agricultural growing season

in Fig. 13. In this figure, most of the SPEI based projections reveal drier conditions over most of the regions in the future. These drier conditions are much stronger over the southern and southwestern regions. Similar results are projected by SPI based analysis, however, with much less severe droughts. The pattern of projected changes to drought duration follows that of drought severity. Also, the projected changes in severity and duration are larger in the growing season than those for the 6-month time scale presented before. Also, the spatial extents of projected changes are larger for the growing season than that of the 6-month time scale. As for the 6-month time scale, the statistical significance of projected changes to mean severity and duration is assessed using the nonparametric vector bootstrap approach. For mean severity and duration, from four to eight RCM_AOGCM pairs suggest significant positive projected changes for most of the southern regions (e.g. Region 9, 11, 12, 13 and 15) and significant negative changes for some of the northern regions (e.g. Region 1, 4 and 5).

The above results specifically for the southern Canadian Prairies region are in general consistent with the findings of Bonsal et al. (2012), who employed statistical downscaling of a few AOGCM outputs, PaiMazumder et al. (2013), who employed a five member ensemble of a single RCM and Gao et al. (2014), who used simulations from the Coupled Model Intercomparison Project Phase 5 GCMs and a high-resolution RCM. Although there are considerable differences in the underlying methodology and simulations used, the patterns of increased dryness are similar.

5 Conclusions

From various analyses presented and discussed in this paper, following main conclusions can be drawn:

1. To facilitate drought risk analysis, the study area is divided into fifteen different geographic regions based on numerous trials of hierarchical clustering. Statistical homogeneity of these regions is verified based on uni- and bivariate homogeneity analysis tests. The bivariate homogeneity test suggests that all regions can be considered homogeneous compared to the univariate test, which identifies a few regions as possibly heterogeneous, particularly for the case of drought duration. Thus, the results of this study highlight the importance of considering simultaneously two highly correlated characteristics of droughts for identifying homogeneous regions. It is interesting to point out that employing homogeneous regions for regional frequency analysis is beneficial in reducing the undesirable noise resulting from grid-based analysis when identifying projected changes to variables of interest.
2. For validating various RCMs, mean drought severity and duration values derived from NCEP-driven RCM simulations are compared with those from the observed data. This comparison indicates that RCMs tend to produce relatively more severe droughts for the central and eastern regions of the study area. The performance errors of RCMs are assessed by comparing selected regional return levels of drought severity and duration. Relative difference between 20- and 50-year return levels derived from NCEP-driven RCM simulations and observed data suggest that the differences are highly model dependent which could be as high as 60 %. However, by considering ensemble-averaged values, relative differences are found to be much smaller than for the individual models for the majority of the regions. The lateral boundary forcing errors are also assessed by comparing selected regional return levels of drought severity and duration derived from NCEP- and AOGCM-driven simulations. It is found that the boundary forcing errors are much smaller than the performance errors for both SPI- and SPEI-based drought severity and duration.
3. Most of the RCM_AOGCM simulations project an increase in drought characteristics for the southern parts of the study area, while some model combinations project completely positive changes for the entire study area. Comparison of analyses based on both SPI and SPEI reveal that the effect of temperature in drought characterization is important for future drought risk analysis and assessment for this region. Similar results are realized for the agricultural growing season, where the drought characteristics are projected to increase with relatively higher margins. Compared to the SPI based projections, SPEI based projections of most of the RCM_AOGCM simulations suggest drier conditions over many parts of the study area, in particular, the southern and south-western regions are found relatively more drought vulnerable. Therefore, considering potential effects from both precipitation and temperature changes is vital for assessing future drought risks. It is also found that from four to eight (out of eleven) RCM_AOGCM pairs suggest significant projected increases (decreases) in drought characteristics for the southern (northern) parts of the study area.
4. Most of the RCM_AOGCM simulations project an increase in return levels of drought severity and duration for southern regions, with some differences noted between models and between different return periods considered. More regions emerge with positive changes in drought characteristics, with higher magnitude of change in return levels corresponding to lower

return period (i.e. 20-year) than higher return period (e.g. 50-year) values. On average, positive changes of up to 60 % are noted for regions located in the southern and south-western parts of the study area. Also, most of the RCM_AOGCM simulation pairs (more than seven) show significant positive (negative) changes in return levels for southern (northern) parts of the study area. However, the number of pairs that are characterized by significant changes is smaller for longer return periods (e.g. 50-year versus 20-year).

5. Projected changes in joint occurrence probabilities of droughts for bi- and trivariate cases are spatially mapped over the study area in order to identify drought vulnerable regions. Overall, central and southern regions are found highly drought vulnerable compared to the northern regions, which are associated with less frequent droughts in the future. For the trivariate case, only one region is found to be highly vulnerable to droughts. The projected changes in joint probabilites (increases for the southern parts and decreases for the northern parts of the study area) for the future period are found statistically significant for the majority of the RCM_AOGCM pairs. Multivariate joint occurrence probabilities from the multivariate drought distribution can describe drought events perhaps closer to the reality and therefore can reveal their properties more objectively and comprehensively. This type of information could serve as a reference for regional drought defense and agricultural resources management purposes.

The results from different models show remarkable influence of the driving AOGCM on the magnitude and sign of the projected change. Perhaps, a single regional climate model cannot describe fully the complex natural climate system, no matter how complex the model itself is. Therefore, combined information from several models can be superior to a single-model output. Besides, according to Tebaldi and Knutti (2007), combining models generally increase the skill, reliability and consistency of model projections. Therefore, it is advisable to consider climate change simulations from numerous models in future drought risk analysis studies in order to derive climate change related information in a robust manner.

The southern parts of the study area are famous for agricultural activities as they support about 80 % of the Canadian agricultural production. These activities are susceptible to extreme climate events like droughts. The economic impacts of droughts can vary depending on how significantly crop production is affected. A mild drought might reduce yields modestly, whereas a more severe drought could produce a total failure of crop production (Wandel et al. 2009). The future climate projections presented in this study suggest droughts will become increasingly common and severe, driven primarily by an increase in *PET*. Therefore, appropriate adaptation strategies at the watershed and regional levels will be required to cope with the drought consequences and aid agricultural managers and water resource planners in their day-to-day activities.

Acknowledgments The authors would like to thank the NARCCAP project team for the RCM simulations and Agriculture and Agri-Food Canada and Eva Mekis, from Environment Canada, for providing the observed datasets. The financial support from the Canada Excellence Research Chair in Water Security and School of Environment and Sustainability, University of Saskatchewan, is also acknowledged. Thanks are also due to Fateh Chebana from Institut national de la recherche scientifique (INRS) for his support with the bivariate homogeneity testing, Seth McGinnis from NARCCAP for the computational support in re-gridding model data, and Amir Sadeghian from the Global Institute for Water Security for help with the spatial maps. We sincerely thank two anonymous referees for their very helpful, logical and constructive comments which helped improve the quality of this paper.

References

Armstrong RN, Pomeroy JW, Martz LW (2015) Variability in evaporation across the Canadian Prairie region during drought and non-drought periods. J Hydrol 521:182–195

Beniston M, Stephenson DB, Christenson OB, Ferro CAT, Frei C, Goyette S, Halsnaes K, Holt T, Jylhä K, Koffi B, Palutikof J, Schöll R, Semmler T, Woth K (2007) Future extreme events in European climate: an exploration of regional climate model projections. Clim Change 81:71–95

Bonsal BR, Aider R, Gachon P, Lapp S (2012) An assessment of Canadian prairie drought: past, present, and future. Clim Dyn. doi:10.1007/s00382-012-1422-0

Caya D, Laprise R (1999) A semi-implicit semi-Lagrangian regional climate model: the Canadian RCM. Mon Weather Rev 127:341

Chebana F, Ouarda TBMJ (2007) Multivariate L-moment homogeneity test. Water Resour Res 43(W08406):1–14

Coles S (2001) An introduction to statistical modeling of extreme values. Springer, London

Collins WD et al (2006) The community climate system model version 3 (CCSM3). J Clim 19:2122–2143

Diasso U, Abiodun BJ (2015) Drought modes in West Africa and how well CORDEX RCMs simulate them. Theor Appl Climatol. doi:10.1007/s00704-015-1705-6

Efron B, Tibshirani RJ (1993) An introduction to the bootstrap. Chapman and Hall, New York

Embrechets P, Lindskog F, McNeil AJ (2003) Modelling dependence with copulas and applications to risk management. In: Rachev ST (ed) Handbook of heavy tailed distributions in finance. Elsevier Science, Amsterdam

Evans E, Stewart RE, Henson W, Saunders K (2011) On precipitation and virga over three locations during the 1999–2004 Canadian Prairie drought. Atmos Ocean 49(4):366–379

Flato GM (2005) The third generation coupled global climate model (CGCM3). http://www.ec.gc.ca/ccmac-cccma/default.asp?n=1299529F-1

Flato G, Marotzke J, Abiodun B et al (2013) Evaluation of climate models. In: Stocker TF, Qin D, Plattner G-K, Tignor M, Allen SK, Boschung J, Nauels A, Xia Y, Bex V, Midgley PM (eds)

Climate change 2013: the physical science basis. Contribution of working group I to the fifth assessment report of the intergovernmental panel on climate change stocker. Cambridge University Press, Cambridge

Ganguli P, Reddy MJ (2013) Evaluation of trends and multivariate frequency analysis of droughts in three meteorological subdivisions of western India. Int J Climatol. doi:10.1002/joc.3742

Gao Y, Fu JS, Drake JB, Liu Y, Lamarque J-F (2012) Projected changes of extreme weather events in the Eastern United States based on a high-resolution climate modeling system. Environ Res Lett 7:044025

Gao Y, Leung LR, Lu J, Liu Y, Huang M, Qian Y (2014) Robust spring drying in the southwestern U.S. and seasonal migration of wet/dry patterns in a warmer climate. Geophys Res Lett 41:1745–1751. doi:10.1002/2014GL059562

Genest C, Rémillard B, Beaudoin D (2009) Goodness-of-fit tests for copulas: a review and a power study. Insu Math Econ 44:199–213

GFDL GAMDT (The GFDL Global Model Development Team) (2004) The new GFDL global atmospheric and land model AM2-LM2: evaluation with prescribed SST simulations. J Clim 17:4641–4673

Giorgi F (2006) Regional climate modeling: status and perspectives. J Phys IV 139:101–118

Gordon C et al (2000) The simulation of SST, sea ice extents and ocean heat transports in a version of the Hadley Centre coupled model without flux adjustments. Clim Dyn 16:147–168

Grell GA, Devenyi D (2002) A generalized approach to parameterizing convection combining ensemble and data assimilation techniques. Geophys Res Lett 29:1693–1697

Grell GA, Dudhia J, Stauffer DR (1993) A description of the fifth-generation Penn State/NCAR Mesoscale Model (MM5). NCAR Tech. Note NCAR/TN-398+1A

Guttman NB (1998) Comparing the palmer drought index and the standardized precipitation index. J Am Water Resour Assoc 34(1):113–121

Halwatura D, Lechner AM, Arnold S (2015) Drought severity-duration-frequency curves: a foundation for risk assessment and planning tool for ecosystem establishment in post-mining landscapes. Hydrol Earth Syst Sci 19:1069–1091

Hargreaves GH, Samani ZA (1982) Estimating potential evapotranspiration. Technical note. J Irrig Drain Eng 108(3):225–300

Hargreaves GH, Samani ZA (1985) Reference crop evapotranspiration from temperature. Appl Eng Agric 1(2):96–99

Hosking JRM, Wallis JR (1997) Regional frequency analysis. Cambridge University Press, Cambridge

Huang S, Krysanova V, Hattermann F (2015) Projections of climate change impacts on floods and droughts in Germany using an ensemble of climate change scenarios. Reg Environ Change 15:461–473. doi:10.1007/s10113-014-0606-z

Hutchinson MF (2004) ANUsplin version 4.3: user guide. The Australian National University, Centre for Resource and Environmental Studies, Canberra, Australia. http://cres.anu.edu.au/outputs/anusplin.php

Jensen ME, Burman RD, Allen RG (eds) (1990) Evapotranspiration and irrigation water requirements. ASCE manual 70. American Society of Civil Engineers, Reston

Jeong DI, Sushama L, Khaliq MN (2014) The role of temperature in drought projections over North America. Clim Change 127(2):289–303

Jones RG, Hassell DC, Hudson D, Wilson SS, Jenkins GJ, Mitchell JFB (2003) Workbook on generating high resolution climate change scenarios using PRECIS. UNDP, New York

Juang H-M, Hong S-Y, Kanamitsu M (1997) The NCEP regional spectral model: an update. Bull Am Meteorol Soc 78:2125–2143

Kao S, Govindaraju RS (2010) A copula-based joint deficit index for droughts. J Hydrol 380:121–134

Kaufman L, Rousseuw PJ (1990) Finding groups in data: an introduction to cluster analysis. Wiley-Interscience, New York

Leung LR, Qian Y, Bian X, Washington WM, Han J, Roads JO (2004) Mid-Century ensemble regional climate change scenarios for the Western United States. Clim Change 62(1):75–113

Ma M, Song S, Ren L, Jiang S, Song J (2013) Multivariate drought characteristics using trivariate Gaussian and Student t copulas. Hydrol Process 27:1175–1190

Madadgar S, Moradkhani H (2013) Drought analysis under climate change using copula. J Hydrol Eng 18:746–759

Masud MB, Khaliq MN, Wheater HS (2015) Analysis of meteorological droughts for the Saskatchewan River Basin using univariate and bivariate approaches. J Hydrol 522:452–466

Maulé C, Helgalson W, McGinn S, Cutforth H (2006) Estimation of standardized reference evapotranspiration on the Canadian Prairies using simple models with limited weather data. Can Biosyst Eng 48:1.1–1.11

Mavromatis T (2007) Drought index evaluation for assessing future wheat production in Greece. Intl J Climatol 27:911–924

May W (2008) Potential future changes in the characteristics of daily precipitation in Europe simulated by the HIRHAM regional climate model. Clim Dyn 30:581–603

McGinn SM (2010) Weather and climate patterns in Canada's Prairies grassland. In: Shorthouse JD, Floate KD (eds) Arthropods of Canadian grasslands (volume 1): ecology and interactions in grasslands habitats. Biological Survey of Canada, Ottawa, pp 105–119. doi:10.3752/9780968932148.ch5

McKee TB, Doesken NJ, Kleist J (1993) The relationship of drought frequency and duration to time scales. In: Preprints 8th conference on applied climatology. American Meteorological Society, Anaheim, CA, pp 179–184

Mearns LO, Gutowski WJ, Jones R, Leung L-Y, McGinnis S, Nunes AMB, Qian Y (2009) A regional climate change assessment program for North America. EOS Trans Am Geophys Union 90:311–312

Mearns LO et al (2012) The North American regional climate change assessment program: overview of phase I results. Bull Am Meteor Soc 93:1337–1362. doi:10.1175/BAMS-D-11-00223.1

Mekis E, Vincent LA (2011) An overview of the second generation adjusted daily precipitation dataset for trend analysis in Canada. Atmos Ocean 49(2):163–177

Mladjic B, Sushama L, Khaliq MN, Laprise R, Caya D, Roy R (2011) Canadian RCM projected changes to extreme precipitation characteristics over Canada. J Clim 24:2565–2584

Mohan S (1991) Intercomparison of evapotranspiration estimates. Hydrol Sci J 36(5):447–461

Nakicenovic N et al (2000) Special report on emissions scenarios: a special report of working group III of the intergovernmental panel on climate change. Cambridge University Press, Cambridge, UK. http://www.grida.no/climate/ipcc/emission/index.htm

Nelsen RB (2006) An introduction to copulas. Springer, New York, p 272

Nikulin G, Kjellström E, Hansson U, Strandberg G, Ullerstig A (2011) Evaluation and future projections of temperature, precipitation and wind extremes over Europe in an ensemble of regional climate simulations. Tellus Ser A 63(1):41–55. doi:10.1111/j.1600-0870.2010.00466.x

PaiMazumder D, Sushama L, Laprise R, Khaliq MN, Sauchyn D (2013) Canadian RCM projected changes to short- and long-term drought characteristics over the Canadian Prairies. Intl J Climatol 33:1409–1423

Pal JS et al (2007) Regional climate modeling for the developing world: the ICTP RegCM3 and RegCNET. Bull Am Meteorol Soc 88:1395–1409

Poitras V, Sushama L, Seglenieks F, Khaliq MN, Soulis E (2011) Projected changes to streamflow characteristics over Western Canada as simulated by the Canadian RCM. J Hydrometeorol 12:1395–1413

Pomeroy J, Pietroniro A, Fang X, Shaw D, Armstrong R, Shook K, Comeau L, Toth B, Martz L, Westbrook C (2011) Canadian prairie drought hydrology. In: Stewart R, Lawford R (eds) Drought research initiative, pp 59–62. ISBN No. 978-0-9868749-0-1

Potop V, Možný M, Soukup J (2012) Drought evolution at various time scales in the lowland regions and their impact on vegetable crops in the Czech Republic. Agric For Met 156:121–133

Rajsekhar D, Mishra AK, Singh VP (2013) Regionalization of drought characteristics using an entropy approach. J Hydrol Eng 18:870–887

Rao AR, Srinivas VV (2008) Regionalization of watersheds—an approach based on cluster analysis. Springer, Berlin

Sadri S, Burn DH (2011) A fuzzy c-means approach for regionalization using a bivariate homogeneity and discordancy approach. J Hydrol 401:231–239

Savu C, Trede M (2010) Hierarchies of Archimedean copulas. Quant Finance 10(3):295–304

Serfling R, Xiao P (2007) A contribution to multivariate L-moments: L-commoment matrics. J Multivar Anal 98:1765–1781

Serinaldi F, Grimaldi S (2007) Fully nested 3-copula: procedure and application on hydrological data. J Hydrol Eng 12(4):420–430

Serinaldi F, Bonaccorso B, Cancelliere A, Grimaldi S (2009) Probabilistic characterization of drought properties through copulas. Phys Chem Earth 34(10–12):596–605

Sklar K (1959) Fonctions de repartition ‘a n dimensions et leura marges. Publications de 1’Institut de Statistique de l’Universit´e, Paris 8, pp 229–231

Stagge JH, Tallaksen LM, Gudmundsson L, Van Loon AF, Stahl K (2015) Candidate distributions for climatological drought indices (SPI and SPEI). Int J Climatol 35:4027–4040. doi:10.1002/joc.4267

Sushama L, Khaliq N, Laprise R (2010) Dry spell characteristics over Canada in a changing climate as simulated by the Canadian RCM. Global Planet Change 74(1):1–14

Tebaldi C, Knutti R (2007) The use of the multi-model ensemble in probabilistic climate projections. Philos Trans R Soc A 365:2053–2075

Torma C, Giorgi F, Coppola E (2015) Added value of regional climate modeling over areas characterized by complex terrain—precipitation over the Alps. J Geophys Res Atmos 120:3957–3972

Touma D, Ashfaq M, Nayak MA, Kao S-C, Diffenbaugh NS (2015) A multi-model and multi-index evaluation of drought characteristics in the 21st century. J Hydrol 526:196–207

Vicente-Serrano SM, Beguería S, López-Moreno JI (2010) A multi-scalar drought index sensitive to global warming: the standardized precipitation evapotranspiration index. J Clim 23(7):1696–1718

Walpole RE, Myers RH, Myers SL, Ye K (2012) Probability & statistics for engineers & scientists. Prentice Hall, Boston

Wandel J, Young G, Smit B (2009) The 2001–2002 drought: vulnerability and adaptation in Alberta’s special areas. Prairie Forum 34(1):211–234

Wang T, Hamann A, Spittlehouse DL, Murdock TQ (2012) ClimateWNA–high-resolution spatial climate data for Western North America. Agric For Met 51:16–29. doi:10.1175/JAMC-D-11-043.1

Wehner M (2013) Very extreme seasonal precipitation in the NARCCAP ensemble: model performance and projections. Clim Dyn 40:59–80. doi:10.1007/s00382-012-1393-1

Wheater HS, Gober P (2013) Water security in the Canadian prairies: science and management challenges. Philos Trans R Soc A. doi:10.1098/rsta.2012.0409

WMO (2009) Inter-regional workshop in indices and early warning systems for drought (Lincoln, NE, Dec. 2009). World Meteorological Organization, Geneva

Wong G, Lambert MF, Leonard M, Metcalfe AV (2010) Drought analysis using trivariate copulas conditional on climate states. J Hydrol Eng 15(2):129–141